Photosynthesis Research **66:** 125–144, 2000.

Emerging techniques

Efficient light harvesting through carotenoids

Thorsten Ritz[1], Ana Damjanović[1], Klaus Schulten[1,*], Jian-Ping Zhang[2] & Yasushi Koyama[2]
[1]*Theoretical Biophysics Group, Beckman Institute, University of Illinois at Urbana–Champaign, Urbana, IL 61801, USA;* [2]*Faculty of Science, Kwansei Gakuin University, Uegahara, Nishinomiya 662, Japan; *Author for correspondence (e-mail: kschulte@ks.uiuc.edu; fax: +1-217-244-6078)*

Received 20 April 2000; accepted in revised form 31 August 2000

Key words: coulomb coupling, excitation transfer, Förster theory, light-harvesting complexes

Abstract

We review the factors that control the efficiency of carotenoid-chlorophyll excitation transfer in photosynthetic light harvesting. For this we summarize first the recently developed theory that describes electronic couplings between carotenoids and chlorophylls and we outline in particular the influence of length of conjugated system and of symmetry breaking on the couplings. We focus hereby on the structurally solved lycopene-BChl system of LH 2 from *Rhodospirillum molischianum* and the peridinin-Chl *a* system of PCP from *Amphidinium carterae*. In addition, we review recent spectroscopic data for neurosporene, spheroidene and lycopene, three carotenoids with different lengths of conjugated systems. On the basis of the measured energies, emission lineshapes, solution and protein environment lifetimes for their $2A_g^-$ and $1B_u^+$ states as well as of the theoretically determined couplings, we conclude that the transfer efficiencies from the $2A_g^-$ state are controlled by the Car($2A_g^-$)–BChl(Q_g) electronic couplings and the $2A_g^- \rightarrow 1A_g^-$ internal conversion rates. We suggest that symmetry breaking and geometry rather than length of conjugated system dominate couplings involving the $2A_g^-$ state. Differences in transfer efficiencies from the $1B_u^+$ state in LH 2 and PCP are found to be dominated by the differences in spectral overlap. The role of the $1B_u^+$ state is likely to be influenced by a lower-lying (in longer polyenes), optically forbidden $1B_u^-$ state.

Introduction

In photosynthetic light harvesting, light absorption through chlorophylls (Chl) is accompanied by light absorption through a second class of chromophores, the carotenoids (Car). The absorbed light energy is then transferred, in the form of electronic singlet excitations, from the carotenoids to the chlorophylls in the light-harvesting complexes which, in turn, transfer it to the photosynthetic reaction center. A second function of carotenoids is photoprotection by quenching chlorophyll triplet states to prevent generation of highly reactive singlet oxygen. The influence of the length and geometry of carotenoids on their photoprotection efficiency has been addressed in several articles, e.g. in Farshoosh et al. (1994), Angerhofer et al. (1995), Young and Frank (1996) and Farshoosh et al. (1997). In the present article, we focus on recent studies of singlet excitation transfer and the light-harvesting function (Koyama et al. 1996; Frank et al. 1997) of carotenoids.

Carotenoids, along with polyenes, have an unusual structure of electronic excitations, a high-lying, absorbing state, which is often labeled according to its symmetry in pure polyenes as $1B_u^+$, and a low-lying, optically forbidden S_1 or $2A_g^-$ state. The discovery of the latter state dates back nearly 30 years (Schulten and Karplus 1972; Hudson and Kohler 1972). The $1B_u^+$ state decays within hundreds of fs into the $2A_g^-$ state. Theory had suggested that there exists another optically forbidden $1B_u^-$ state between the $1B_u^+$ and $2A_g^-$ state for carotenoids (polyenes) with six or more conjugated double bonds (Tavan and Schulten 1987), which has recently been observed in experiments (Sashima et al. 1999, 2000). The discovery of this new state requires a relabeling of the states. The

$1B_u^+$ state, which had been denoted as the S_1 state before 1972, then the S_2 state, is now realized to be often the third excited, i.e. S_3, state, while a $1B_u^-$ is the S_2 state. We will adopt this new notation throughout our article. Since this notation is unfamiliar, we will in addition frequently refer to the polyene labels to avoid confusion.

The overall transfer efficiencies for Car → Chl transfer have been measured by fluorescence excitation spectroscopy, showing a variability between different species and light-harvesting complexes. The overall transfer efficiency is close to 100% in *Rhodobacter (Rb.) sphaeroides* (Cogdell et al. 1981; Van Grondelle et al. 1982; Kramer et al. 1984; Trautmann et al. 1990), between 38–75% in *Rhodopseudomonas (Rps.) acidophila* (Augerhofer et al. 1986; Chadwich et al. 1987; Cogdell et al. 1992), and as low as 30% in LH-1 of *Rhodospirillum (Rs.) rubrum* (Frank 1993). The differences in efficiencies have not yet found a satisfactory explanation.

An obvious suggestion is that species with high transfer efficiencies can utilize transfer through the optically forbidden S_1 state, while those with lower efficiencies cannot. There are three factors that can in principle account for the differences in transfer efficiencies for different carotenoid-chlorophyll systems: The electronic coupling between the donor carotenoid and acceptor Chl state, the spectral overlap of donor emission and acceptor absorption spectra, and the lifetime of the donor state in the absence of energy transfer. The first two factors determine the energy transfer rate, which depends quadratically on the electronic coupling and linearly on the spectral overlap. The third factor determines the transfer efficiency because energy transfer has to compete with internal conversion in the donor.

The carotenoid S_3 and S_1 excited states are in resonance with Chl Q_x and Q_y excitations, thus allowing two different transfer pathways, $S_3 \rightarrow Q_x$ transfer, and $S_1 \rightarrow Q_y$ transfer. The transfer time for Car → Chl transfer has been measured or estimated to be in the range of 100–250 fs, which is on the order of the S_3 ($1B_u^+$) state lifetime. This means that the overall efficiency should be in the range of 30–70% if it were solely based on $S_3(1B_u^+) \rightarrow Q_x$ transfer. Species with near unit transfer efficiencies have to utilize the $S_1 \rightarrow Q_y$ pathway in addition. The question we seek to answer in the present publication is why $S_1 \rightarrow Q_y$ transfer is efficient in some species but not in others.

Our understanding of the mechanism of energy transfer between carotenoids and chlorophylls has been greatly advanced by the recent high-resolution crystal structures of LH 2 from two species of purple bacteria, *Rps. acidophila* and *Rs. molischianum* (McDermott et al. 1995; Freer et al. 1996; Koepke et al. 1996). In addition, a high-resolution structure of the light-harvesting system peridinin–chlorophyll–protein (PCP) from the dinoflagellate *Amphidinium (A.) carterae*, in which carotenoids are the more abundant light absorbers, has been solved (Hofmann et al. 1996). The crystal structures provide information on the geometrical details of the arrangement of carotenoids and chlorophylls. This information would be of little value without a theory that allows one to evaluate the electronic couplings mediating excitation transfer on the basis of the geometry of the molecules involved.

The well-known Förster theory (Förster 1948, 1965) determines the geometry dependence of excitation transfer under the assumption that the relevant interaction between donor and acceptor can be approximated by the leading dipole–dipole term. This approximation is valid when the extension of the molecules involved is small compared to the distance between the molecules. In the case of Car → Chl transfer, the extension of the molecules (about 20 Å for carotenoids) is about as large as the distance between the molecule centers (about 15 Å) and larger than the distance between closest atoms (between 3 Å and 6 Å depending on the species and the Car–Chl pair) and one needs to account for the full Coulomb coupling without invoking a multipole approximation.

The necessary calculations are computationally challenging since they require knowledge of the wavefunctions of the highly correlated electron system of carotenoids and chlorophylls. Several groups have developed methods to calculate the full Coulomb coupling; e.g. in Nagae et al. (1993). The transition density cube method of the Fleming group (Krueger et al. 1998a, b; Scholes et al. 1999) and the evaluation of transition density matrix elements developed independently by the Schulten group (Ritz et al. 1998a; Damjanović et al. 1999) are both recent methods that follow the spirit of the work of Nagae et al. (1993). With these methods, it is now possible to evaluate the geometry dependence of the electronic coupling without the approximations inherent in Förster theory.

The full Coulomb coupling theory is less intuitive than the Förster theory since one has to take into account many different transition matrix elements that cancel each other partly. Even in the case of transfer between optically allowed states, the orientation

of transition dipole moments does not allow any predictions about the strength of the coupling, since the dipole–dipole term does not necessarily give the leading contribution to the couplings. As an analysis in Krueger et al. (1998b) shows, the full Coulomb coupling can differ by up to a factor of four from the Förster dipole–dipole coupling term, i.e. an estimate of the transfer rate based solely on the transition dipole contribution would differ up to 16 times from the correct transfer rate evaluated on the basis of the full Coulomb coupling.

Transfer from the optically forbidden S_1 state cannot occur via the Förster mechanism which requires the participating states to be allowed. It had been suggested that excitation transfer from this state can occur via the Coulomb mechanism (Thrash et al. 1979). Alternatively, the electron exchange (Dexter) mechanism (Dexter 1953) had been suggested to mediate transfer through the S_1 state (Naqvi 1980; Gillbro et al. 1988). The relative sizes of the couplings through the electron exchange and through the Coulomb interaction term have been evaluated with all of the above mentioned full Coulomb coupling methods. These calculations show that the Dexter mechanism depends sensitively on edge-to-edge chromophore distances and is inefficient compared to the full Coulomb coupling mechanism even if the forbidden S_1 state is involved. This result has been ascertained for Car–Chl contacts in the range found in light harvesting, regardless of the details of the calculation method and has been found valid not only for a systematic study of hypothetical carotenoid-chlorophyll arrangements (Nagae et al. 1993), but also for the calculations based on the crystal structures of LH 2 from *Rps. acidophila* (Krueger et al. 1998b), of LH 2 from *Rs. molischianum* (Damjanović et al. 1999) and PCP from *A. carterae* (Damjanović et al. 2000b).

In this article, we provide an overview over the recently developed full Coulomb coupling methods. While these methods allow one to calculate electronic couplings for energy transfer without the approximations made in the Förster theory, inaccuracies in the evaluation of the excited state wavefunctions lead to errors in the calculation of electronic couplings.

Nevertheless, after *a posteriori* scaling of electronic couplings with a factor derived from the ratio between calculated and experimentally measured transition dipole moments, the calculated transfer rates were found to agree closely with experimentally observed transfer rates (Krueger et al. 1998b). We will discuss below that such agreement should not be expected from a theoretical standpoint. Further studies, assessing the accuracy and limitations of full Coulomb coupling methods, are needed to determine whether this agreement is merely fortuituous or the result of a deeper, not yet understood, principle. In parallel, methods to evaluate wavefunctions that are optimized for the needs of full Coulomb coupling methods, should be developed in order to overcome the current quantitative shortcomings of these methods.

Rather than employing the questionable scaling of electronic couplings, we use the full Coulomb coupling method to discuss, in a qualitative manner, the influence of the number of conjugated double bonds and the influence of breaking of the polyene symmetry on the electronic couplings. We compare the results from calculations to the experimentally observed energy gap laws. In particular, we show that geometric distortions of the polyene symmetry within the protein environment strongly increase electronic couplings with the S_1 state.

The advances in theoretical methods, which now allow one to evaluate, at least qualitatively, the differences in electronic couplings for different carotenoids, are paralleled by no less exciting experimental advances. For a long time, carotenoid fluorescence spectra could not be measured for the S_1 state of carotenoids with more than nine conjugated double bonds. Recently, three groups succeeded in determining S_1 state energies of long carotenoids. The Sundström group measured the zeaxanthin and violaxanthin S_1 energies through a femtosecond transient absorption technique (Polivka et al. 1999), the Fleming group measured spheroidene S_1 absorption through two-photon fluorescence excitation (Krueger et al. 1999). An improved fluorescence spectral setup enabled the Frank group to determine S_1 emission energies for violaxanthin and zeaxanthin (Frank et al. 2000a) directly from fluorescence spectroscopy. The Koyama group determined S_1 energies, spectral lineshapes, and transition dipole moments through an improved fluorescence spectral setup and through resonance-Raman excitation spectroscopy for lycopene, spheroidene, and neurosporene (Fujii et al. 1998; Sashima et al. 1998). In addition, the S_1 and S_3 ($1B_u^+$) state lifetimes of these carotenoids in solution and in the protein environment of LH 2 have also been measured recently through transient absorption techniques (Zhang et al. 2000).

These new experimental results, together with the development of full Coulomb coupling methods, provide new and vastly improved information for all

three factors that determine excitation transfer efficiencies in carotenoid-chlorophyll systems: (1) the electronic couplings, (2) the spectral overlap between carotenoid and chlorophyll states, and (3) the lifetimes of carotenoid states. This makes possible for the first time a comprehensive discussion of excitation transfer efficiencies incorporating the influence of all three of the above factors. This advances the pictures presented in recent reviews (Frank and Cogdell 1996; Cogdell et al. 1999; Sundstrom et al. 1999; Christensen 1999), thus making a new overview over this topic necessary. Finally, the above mentioned experimental verification of a new low-lying, optically forbidden S_2 ($1B_u^-$) state (Sashima et al. 1999, 2000) is a new result that changes our picture of the carotenoid energy structure significantly. We can at this moment only point to open questions raised by the existence of this state, since its implications for excitation transfer have yet to be studied.

Full Coulomb coupling

The rate of excitation transfer from a donor chromophore to an acceptor chromophore can be evaluated by means of the well-known expression

$$k_{DA} = \frac{2\pi}{\hbar}|U_{DA}|^2 J_{DA}. \tag{1}$$

Here, U_{DA} describes the electronic coupling between donor and acceptor states, J_{DA} is the overlap integral between the spectra of donor emission $S_D(E)$ and acceptor absorption $S_A(E)$, for which the intensity (area) has been normalized to 1,

$$J_{DA} = \int \frac{S_D(E)\ S_A(E)}{E^4}\, dE\ . \tag{2}$$

The function of the spectral overlap term J_{DA} is to ensure energy conservation by evaluating the fraction of donor and acceptor states that are in resonance. For most carotenoid–chlorophyll systems, the energy origin and lineshape of the spectra can be estimated from spectroscopic measurements. A notable exception occurs in the case of transfer to the B850 bacteriochlorophyll (BChl) ring in LH 2. Because of the strong coupling between the individual B850 BChls, delocalized exciton states are formed. Of these, only one pair of degenerate states carries large oscillator strength and only this pair of states can be observed through spectroscopy. Calculations are required to determine the energies (Hu et al. 1997) and lineshapes (Mukai et al. 1999) of the optically forbidden exciton states. In the case of B800 $\rightarrow$ B850 excitation transfer, it has been shown that transfer rates are enhanced because of the large spectral overlap of the high-lying B850 exciton states with the B800 Q_y state (Hu et al. 1997; Ritz et al. 1998b; Sumi 1999). It has been suggested that carotenoid-chlorophyll transfer rates can also be enhanced through these states, albeit to a lesser extent than for B800 $\rightarrow$ B850 transfer (Damjanović et al. 1999).

The electronic coupling U_{DA} can be either a Coulomb or an exchange coupling term. Electron exchange terms rely on overlap between donor and acceptor orbitals and decay exponentially with increasing distance between donor and acceptor. The Dexter electron exchange coupling (Dexter 1953) has been evaluated for various carotenoid–chlorophyll systems (Nagae et al. 1993; Krueger et al. 1998a, b; Damjanović et al. 1999, 2000b) and was very small compared to the Coulomb coupling in all cases. The Dexter coupling describes a simultanous exchange of electrons. An alternative to the Dexter exchange coupling is an exchange coupling that is mediated through successive virtual one-electron transfers to and from an intermediate ionic configuration. It has been suggested by several authors (Scholes et al. 1995, 1997, 1999) that the latter exchange coupling is larger than the Dexter exchange coupling, however, it was still found to be smaller than the Coulomb coupling.

In the following, we will, therefore, neglect the effects of exchange coupling on transfer between carotenoid and chlorophyll singlet states. The electronic coupling U_{DA} can then be expressed as

$$\begin{aligned} U_{DA} =& U_{DA}(\text{elec}) \\ &+ U_{DA}(\text{pol}) + U_{DA}(\text{disp}) + U_{DA}(\text{res})\ . \end{aligned} \tag{3}$$

Here, U_{DA}(elec) is the electrostatic interaction, U_{DA}(pol) the polarization energy, U_{DA}(disp) the dispersion energy and U_{DA}(res) the resonance energy. The terms U_{DA}(pol) and U_{DA}(disp) have been suggested to play a role in carotenoid $S_1 \rightarrow$ Chl excitation transfer (Scholes et al. 1997); their role is supported by experiments (Herek et al. 1998) that reveal a change in carotenoid spectra upon excitation of BChls. In the present article, we neglect these effects and assume that the resonance energy U_{DA}(res) is the dominant contribution to U_{DA}.

U_{DA}(res) can be expressed as (McWeeny 1992) (Equation 14.6.8)

$$U_{DA}(res) = \frac{e^2}{4\pi\epsilon_0} \int \frac{P_D(dd'|\vec{r}_1)\, P_A(a'a|\vec{r}_2)}{r_{12}}\, \mathrm{d}\vec{r}_1 \mathrm{d}\vec{r}_2 \,. \qquad (4)$$

Here, the primes denote excited states of donor and acceptor, and $P_{D(A)}$ is the transition density connecting the donor (acceptor) excited and ground states. Using the language of second quantization (Damjanović et al. 1999), one can express Equation (4) as:

$$U_{DA}(\mathrm{res}) = 2 \sum_{\substack{i,j \\ \in I_D}} \sum_{\substack{R,S \\ \in I_A}} (\phi_i\phi_j|\phi_R\phi_S) \times \langle\Psi'_D|^{00}\hat{Q}^i_j|\Psi_D\rangle\ \langle\Psi_A|^{00}\hat{Q}^R_S|\Psi'_A\rangle \qquad (5)$$

Here, $(\phi_i\phi_j|\phi_R\phi_S)$ denotes the Coulomb integral between the non-orthogonal atomic orbitals ϕ_i, ϕ_j on the donor and ϕ_R, ϕ_S on the acceptor:

$$(\phi_i\phi_j|\phi_R\phi_S) = \frac{e^2}{4\pi\epsilon_0} \int \phi'_i(1)\,\phi_j(1)\,\frac{1}{r_{12}}\,\phi'_R(2)\,\phi_S(2)\,\mathrm{d}\vec{r}_1\,\mathrm{d}\vec{r}_2 \,. \qquad (6)$$

$^{00}\hat{Q}^i_j$ and $^{00}\hat{Q}^R_S$ in Equation (5) are the spin tensor operators coupling the ground states to the singlet excited states in a non-orthogonal atomic orbital basis.

Equation (5) shows that the task of evaluating U_{DA} breaks down into summing up many Coulomb integrals with their corresponding transition density matrix elements as coefficients. Coulomb integrals can be evaluated with very high accuracy. If the N-electron wavefunctions $\Psi_{D(A)}(\vec{x}_1, \vec{x}_2, \ldots, \vec{x}_N)$, $\Psi'_{D(A)}(\vec{x}_1, \vec{x}_2, \ldots, \vec{x}_N)$ could be evaluated exactly, Equation 4 would allow exact (except for the neglect of orbital overlap contributions) evaluation of the full Coulomb interaction energy between the states $|\Psi'_D\Psi_A\rangle$ and $|\Psi_D\Psi'_A\rangle$, using the geometries from the crystal structures as input. However, the excited state wavefunctions $\Psi'_{D(A)}$ for the conjugated systems of 9–12 π electrons, as found in carotenoids and BChls involved in light harvesting, can only be solved approximately, thus resulting in an error in the evaluation of U_{DA}.

The excited state wavefunctions are typically evaluated using a configuration interaction (CI) approach. For this purpose, a basis is constructed that is restricted to single (CI-S), single + double (CI-SD), and subsequently higher configurations to provide a framework for the solution of the eigenvalue problem of the Hamiltonian for carotenoids and chlorophylls. The methods in Krueger et al. (1998b) and Damjanović et al. (1999) differ in the size of the basis set and the choice of the Hamiltonian. The authors in Krueger et al. (1998b) use a (CI-S) basis set and an *ab initio* Hamiltonian. The authors in Damjanović et al. (1999) employ a (CI-SD) basis set for the carotenoid states and a semiempirical Pariser-Parr-Pople Hamiltonian. For a complete basis set, the *ab initio* Hamiltonian yields exact results for the wavefunctions while the semi-empirical Hamiltonian will result in an approximate wavefunction. However, semi-empirical Hamiltonians are often parametrized to reproduce experimental energy values for restricted basis sets and are, arguably, as good as or better than *ab initio* Hamiltonians for evaluating Coulomb couplings in restricted basis sets. The CI-S basis set can be used to approximate the BChl states and the carotenoid S_3 ($1B_u^+$) state. The carotenoid S_1 ($2A_g^-$) and S_2 ($1B_u^-$) states, however, are dominated by double excited configurations (Schulten et al. 1976) and require at least a CI-SD basis set or a treatment with multireference CI methods (Tavan and Schulten 1979; Tavan and Schulten 1986).

The symmetries of the electronic states and corresponding wavefunctions are reflected in the transition density matrix elements. As long as carotenoids obey approximately the polyene C_{2h} and alternancy symmetries, selection rules for the transition densities can be stated (Damjanović et al. 1999), which allow one to explain the coupling strengths. Below, we will discuss how the breaking of the polyene symmetries can be instrumental in enhancing transfer through the S_1 state of carotenoids.

The coupling U_{DA}(res) can be evaluated without resorting to the language of second quantization, by evaluating transition densities between ground states Ψ and excited state Ψ' for donor and acceptor in sufficiently small three-dimensional volume elements (cubes) and then summing over these transition density cubes:

$$\tilde{P}(\vec{r}) = V_\delta \int_z^{z+\delta_z} \int_y^{y+\delta_y} \int_x^{x+\delta_x} \int_s \Psi(\vec{r}, s)\Psi'^*(\vec{r}, s) ds d\vec{r} \,, \qquad (7)$$

where s represents the spin variables, the δ_α denote the grid size and $V_\delta = \delta_x\delta_y\delta_z$ is the element volume, needed as a practical means of converting charge density per unit volume into charge density per element. Such an evaluation of transition density cubes can

be performed with the quantum chemistry program package Gaussian94 as explained in Krueger et al. (1998b).

Transition dipole moments: Relation to Förster theory

The expression of U_{DA} in Equation (4) contains a r^{-1} dependence on the intermolecular distance r, whereas Förster's resonance term contains a r^{-3} term (leading to the inverse sixth power when evaluating rates). The familiar r^{-3} dependence arises if one approximates Equation (4) by only the dipole–dipole term in the interaction

$$U^{dd} = \frac{\vec{\mu}_D \vec{\mu}_A}{|r_{DA}^3|} - \frac{3(\vec{\mu}_D \vec{r}_{DA})(\vec{\mu}_A \vec{r}_{DA})}{|r_{DA}^5|} \,. \tag{8}$$

Here, $\vec{r}_{DA}$ denotes the vector between the centers of the donor and acceptor molecules $\vec{\mu}_{D(A)}$ are the transition dipole moments related through the transition densities according to

$$\mu_D = \langle \Psi_d' | \sum_{i=1}^{N} e\, \vec{r}_d^{\,i} | \Psi_d \rangle = \sum_{i=1}^{N} e\, \vec{r}_d^{\,i} P(dd'|\vec{r}_d^{\,i}) \,. \tag{9}$$

Such an approximation is acceptable if the distance $|r_{d(a)}^i|$ of atom i from the donor (acceptor) to the center $\vec{r}_{D(A)}$ of the donor (acceptor) molecule is small compared to the distance $|r_{DA}|$ between the centers of both molecules. This is, however, not the case in the case of carotenoid–chlorophyll transfer, where the size of the two molecules is actually large in comparison to their center-to-center distances, thus, requiring the inclusion of the full Coulomb coupling as described in the section above.

The transition dipole moments $\vec{\mu}_D$ can be measured experimentally which allows one to estimate the error in the evaluation of the transition densities $P(dd'|\vec{r}_1)$ for the donor and analoguously for the acceptor, that are the basis for evaluating the couplings. Typically, the calculated transition dipole moments $\vec{\mu}_D^{calc}$ reported in Krueger et al. (1998b) and Damjanović et al. (1999) differ by up to 50% from the experimental values for the chlorophyll states, while they are within 15% of the experimental values for the carotenoid S_3 states. The transition dipole moment of the forbidden carotenoid S_1 state is too small to be amenable to direct measurement. We discuss below how such a small transition dipole moment can arise and compare results from calculations to estimates from experimental data. For transfer from the S_3 state the above errors would give rise to an error by a factor of three in the transfer rate.

In order to correct for this error, it has been suggested by Krueger et al. (1998b) and Scholes et al. (1999) that to scale the calculated Coulomb couplings U_{DA}^{calc} relative to the experimental transition moments, i.e., to express

$$U_{DA}^{scaled} = U_{DA}^{calc} \frac{|\mu_D^{exp}|}{|\mu_D^{calc}|} \frac{|\mu_A^{exp}|}{|\mu_A^{calc}|} \,. \tag{10}$$

Such a scaling would correct an error in the dipole-dipole interaction term U^{dd} of Equation (8). The question is whether it is also reasonable to scale the complete Coulomb coupling U_{DA} in this way. Obviously, if one can assume that the leading term in the multipolar expansion is the dipole–dipole term, rescaling this term will correct the Coulomb coupling. However, if this assumption were to hold, it would be unnecessary to apply a full Coulomb coupling method; one could just use Förster theory instead. This assumption applies for example when treating excitation transfer between B800 and B850 BChls in LH 2, or between the BChls in LH 1 and the photosynthetic reaction center. In these systems, the distance between donor and acceptor BChls is large enough so that the dipole–dipole term is dominant. If one evaluates the electronic states of the ring systems through a semi-empirical CI-S method, as in Cory et al. (1998), then the couplings will be overestimated. In this case, it is justifiable to scale the couplings according to Equation (10) as presented for LH 1 → RC transfer in Damjanović et al. (2000a).

Discarding the possibility of a dominant dipole–dipole term, the scaling in Equation (10) assumes that *all* terms in the multipolar expansion of U_{DA} scale in the same way as the dipole–dipole term. There is no reason why this should be the case; rather, the definition of higher terms in the multipolar expansion suggests the need for a different scaling factor for each of the higher order multipole terms.

We do not think that the scaling suggested in Equation 10 is justifiable to correct for errors in the full Coulomb coupling and, therefore, we do not employ it. However, we note that such scaling has been applied repeatedly yielding very good agreement between calculated and experimentally measured transfer rates. As stated in the 'Introduction', a theoretical study of this matter, for example in a few-electron system, is urgently needed to determine whether such agreement is merely fortuitous or whether there are conditions under which such agreement is to be expected. Simultaneously, one should investigate whether better parametrization of a semi-empirical Hamilto-

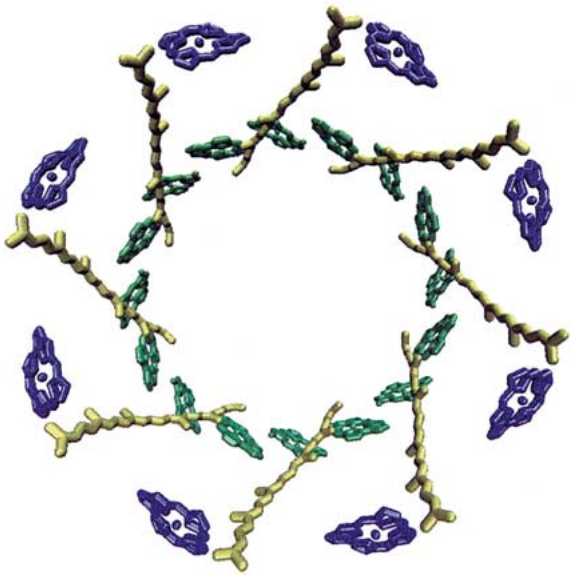

Figure 1. Arrangement of chromophores in LH2 from *Rs. molischianu* in a top view. The coordinates were taken from the crystal structure (Koepke et al. 1996). One can discern the outside ring of B800 BChls (blue) and the closely spaced inside ring of B850 BChls (green). The phytol tails of the BChls have been truncated for clarity. The lycopenes (yellow) stretch through the membrane region, coming in close contact with B800 and B850 BChls. The figure was produced with VMD (Humphrey et al. 1996).

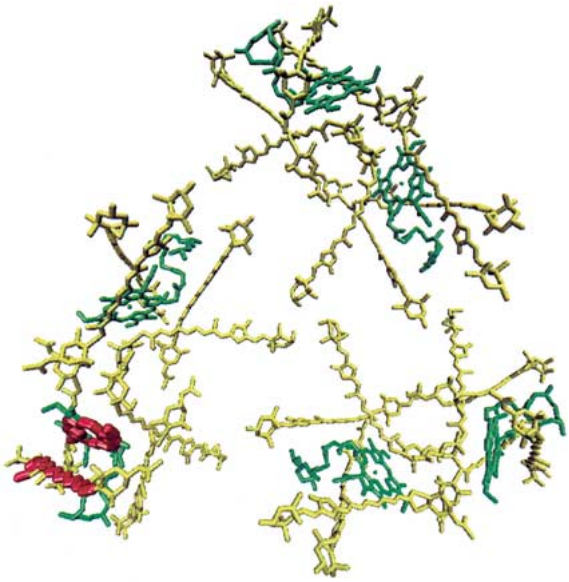

Figure 3. Arrangement of chromophores in PCP from *A. carterae*. The coordinates were taken from the crystal structure (Hofmann et al. 1996). One can discern the 4:1 ratio of carotenoids (peridinin, shown in yellow) to chlorophylls (shown in green). The conjugated systems of peridinin 614 and Chl 601, used in the Coulomb coupling calculations, are highlighted in the lower left monomeric subunit in red. The figure was produced with VMD (Humphrey et al. 1996).

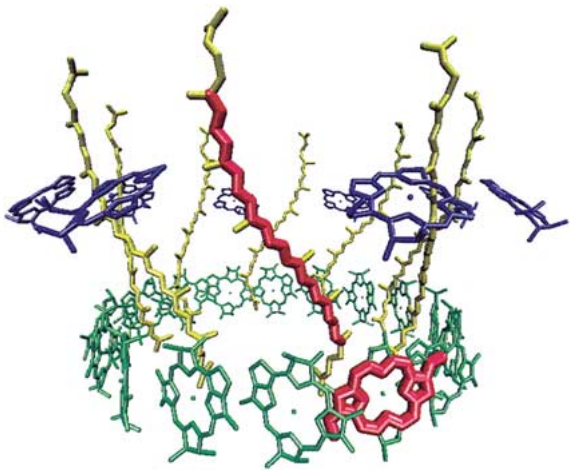

Figure 2. Conjugated systems (in red) of lycopene and B850*a* BChl, used in the Coulomb coupling calculations. For better orientation, the other chromophores in the LH2 complex are also shown in yellow (lycopenes), blue (B800 BChls), and green (B850 BChls) licorice representation with the phytol tails of the BChls truncated for clarity. The figure was produced with VMD (Humphrey et al. 1996).

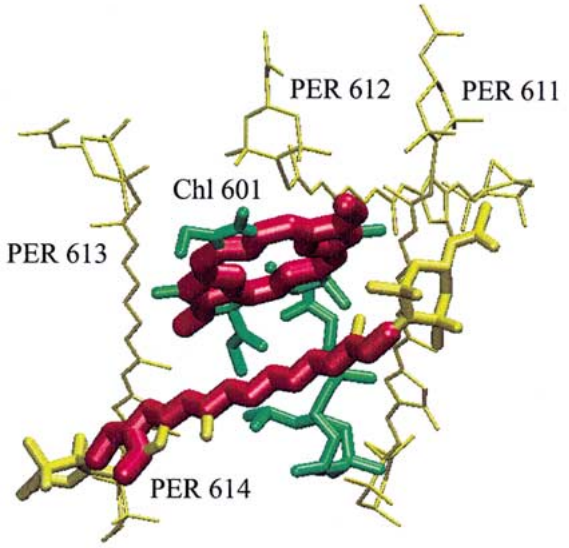

Figure 4. Close-up of the conjugated system (in red) of peridinin 614 and Chl 601, used in the Coulomb coupling calculations. The non-conjugated regions of Chl 601 (green) and the four closest peridinins (yellow) are depicted in licorice representation. The figure was produced with VMD (Humphrey et al. 1996).

nian or CI methods can lead to improved carotenoid and chlorophyll excited state wavefunctions that make a scaling obsolete.

Given the large possible error without scaling of up to a factor of three for the transfer rates, one may ask what one can learn currently from full Coulomb coupling methods. To answer this, we first note that the error of the full Coulomb coupling methods results from a neglect of electron correlation through higher order configurations in the evaluation of the excited state wavefunctions. The error is, therefore, systematically linked to the nature and symmetry of the excited state in question and expected to be approximately of the same magnitude and direction for one given type of excited state. Therefore, the full Coulomb coupling methods allow one to compare electronic couplings for, e.g. different numbers of conjugated double bonds with reasonable accuracy, thus revealing the influence of this property. Even though the full Coulomb coupling methods are not yet accurate enough to reproduce experimental transfer rates, respective calculations can still shed light on the principles governing Car → Chl excitation transfer.

The effect of electronic coupling

Only three structurally resolved carotenoid–chlorophyll systems are amenable to a calculation of the full Coulomb coupling as described in the last section, the lycopene-BChl system from *Rs. molischianum*, the rhodopin glucoside-BChl system from *Rps. acidophila*, and the peridinin–Chl *a* system of *A. carterae*. Of these, the lycopene and rhodopin glucoside systems bear many similarities. The conjugated system of the carotenoids encompasses 11 double bonds and all non-hydrogen sidegroups are arranged in a symmetric fashion. In both systems, the overall transfer efficiency has been shown to be less than unity with the energy transfer being almost exclusively mediated through the S_3 state. Because of these similarities, we will use only one of these two systems as a representative for the following discussion, namely the lycopene–BChl system, on which the authors in this article have focussed their research so far.

The arrangement of chromophores in LH 2 from *Rs. molischianum* is shown in Figures 1 and 2. Figure 1 shows the overall arrangement of chromophores in a top view, Figure 2 shows a closeup of the conjugated system of lycopene and B850*a* BChl, which were used for the calculation of the full Coulomb coupling.

In contrast to the lycopene–BChl system, the peridinin–Chl *a* system shows a near unity transfer efficiency which is almost completely mediated through the S_1 state (Mimuro et al. 1992; Bautista et al. 1999a). Peridinin has 9 conjugated double bonds, a carbonyl group at one end of the conjugated system and asymmetrically arranged methyl groups, strongly disrupting the polyene symmetry. The arrangement of chromophores and a close-up of the peridinin–Chl pair used in our Coulomb coupling calculations are shown in Figures 3 and 4, respectively.

In addition to these two structurally known systems, much can be learned form studying perfect polyenes for which the effects of changes in the number of conjugated double bonds, n, and the effects of symmetry breaking can be studied separately.

S_1 ($2A_g^-$) state

We first investigate the dependence of the $2A_g^-$-Q_y couplings on n, by calculating the couplings between carotenoid analogs and BChl with a full Coulomb coupling method at the CI-SD level. The carotenoid analogs are perfect polyenes with $n = 6$ to $n = 11$. We chose to arrange the polyenes such that their center of mass matches the center of mass of lycopene in LH 2 from *Rs. molischianum* and their axis is aligned at the same angle as the axis of lycopene. The results for the S_1-Q_y couplings show no obvious correlation to the number of conjugated double bonds as can be seen in Table 1, although it can be observed that the smallest couplings occur for the largest n.

It should be noted that the exact geometry is only known for the lycopene–BChl system of LH 2 from *Rs. molischianum*. The placement of the shorter lycopene analogs may result in geometries that are different from the actual carotenoid–BChl geometries in the respective native systems. Coulomb couplings for carotenoid–chlorophyll systems are very sensitive to changes in the geometry of the chromophores. A translation of the polyene by as little as 0.5 Å or a rotation by about 10° can result in changes of a factor two in the couplings (Nagae et al. 1993). This high sensitivity suggests that the variation of couplings seen in Table 2 is a result of geometrical differences rather than changes of the electronic structure due to different lengths of conjugated systems. It also suggests that knowledge of the actual geometries is required for a reliable estimate of electronic couplings and transfer rates.

Table 1. $2A_g^-$–Q_g electronic couplings (in cm^{-1}) calculated for perfect polyenes fitted into the geometries of the lycopene-BChl system in LH 2 from *Rs. molischianum*. The couplings are calculated through the full Coulomb coupling method at the CI-SD level

n	6	7	8	9	10	11
U_{DA}	16.7	26.0	24.3	34.5	2.4	1.6

Table 2. Transition dipole moments (in Debye) derived from fluorescence spectra of the respective states as reported in Zhang et al. (2000)

Carotenoid (n)	μ_{S3}	μ_{S1}	μ_{S1}/μ_{S3} (%)
Neurosporene (9)	14.760	0.856	5.8
Spheroidene (10)	15.646	0.720	4.6
Lycopene (11)	16.377	0.635	3.9

So far, only polyenes with perfect symmetry have been investigated. For polyenes, the transition dipole moment of the $2A_g^-$ state is zero. In carotenoids, the perfect polyene symmetry is broken. Nevertheless, the resulting S_1 transition dipole moment is too weak to be directly measured. However, S_1 emission has been observed recently in several carotenoids (Fujii et al. 1998; Zhang et al. 2000). From the ratio of quantum yield from the fluorescence spectra of S_1 and S_3 together with the lifetimes and energies of the two states, the transition dipole moments can be estimated as described in Zhang et al. (2000). The experimentally measured S_3 transition dipole moments, the estimated S_1 transition dipole moments, and the ratio between them are listed in Table 2.

In order to estimate the effect of an increase in number of double bonds in carotenoids with broken polyene symmetries, we resort to the following consideration. While the S_1 state in perfect polyenes is of $2A_g^-$ symmetry, the S_1 state of carotenoids is a mixture of states of $2A_g^-$ and $1B_u^+$ symmetry.

$$(S_1) \;=\; \alpha\;(2A_g^-) \;+\; \beta\;(1B_u^+) \qquad (11)$$

Because of the orthonormality relations between the states, it holds that $\alpha = \sqrt{1-\beta^2}$. Only the $1B_u^+$ state carries a transition dipole moment. If one assumes that the S_3 state has pure $1B_u^+$ character, the ratio between transition dipole moments of S_1 and S_3 state, given in Table 2, equals β, the fraction of the $1B_u^+$ state which is mixed into the S_1 state. The coupling of the carotenoid S_1 state to the BChl Q_g state can then be calculated as:

$$U_{DA}(S_1 - Q_y) = \sqrt{1-\beta^2}\;U_{DA}(2A_g^- - Q_y) + \beta\;U_{DA}(1B_u^+ - Q_y)\;. \qquad (12)$$

Table 3. Electronic couplings (in cm^{-1}) calculated for perfect polyenes fitted into the geometries of the lycopene-BChl system in LH 2 from *Rs. molischianum*. The $2A_g^-$–Q_y and $1B_u^+$–Q_y couplings are calculated directly through the full Coulomb coupling method at the CI-SD level. Assuming that the S_1 state is a mixture between $2A_g^-$ and $1B_u^+$ states, the S_1–Q_y coupling can be evaluated as a linear combination of the $2A_g^-$–Q_y and $1B_u^+$–Q_y couplings, according to Equation (12). The fraction of the couplings to the pure polyene states that contributes to the mixed S_1–Q_y coupling is indicated in square brackets.

n	U_{DA} ($2A_g^-$–Q_y)	U_{DA}($1B_u^+$–Q_y)	U_{DA}(S_1–Q_y)
9	34.5 [33.5]	134.9 [7.8]	41.3
10	2.4 [2.3]	296.0 [13.6]	15.9
11	1.6 [1.6]	263.8 [12.4]	14.0

As can be seen from Table 3, the mixing of the $1B_u^+$ state contributes between 7.8 and 13.6 cm^{-1} to the overall S_1–Q_y coupling. If the contribution from the $2A_g^-$ state is small, as for long carotenoids, the $1B_u^+$–Q_y coupling contribution becomes dominant, ensuring that the S_1–Q_y coupling does retain a significant value even for longer carotenoids. The overall trend of the S_1–Q_y coupling for an increase in n is difficult to predict because of the varying influence of the many factors involved. We note, however, that the coupling decreases from neurosporene ($n=9$) to lycopene ($n=11$), carotenoids for which we evaluated all the contributing factors.

In order to account for the effect of symmetry breaking more directly, one can distinguish atoms of the conjugated system with functional groups attached from those with hydrogen bonds attached. The atoms with functional groups are treated as heteroatoms, i.e. their parameters entering the calculation of the excited state wavefunctions are altered to incorporate the influence of the functional group (Damjanović et al. 2000b). Instead of using polyene geometries, we use the exact geometries as known from the crystal structures to evaluate S_1–Q_y couplings for the peridinin–chlorophyll and lycopene–BChl systems.

The results of the calculations are very sensitive to the chosen parametrization of the heteroatoms as pointed out in Damjanović et al. (2000b). A test for the quality of the parametrization (and thus the wave-

functions) is to compare the calculated with the experimentally observed transition dipole moment. For lycopene, the calculated transition dipole moment for the S_1 state with heteroatom parametrization is 0.55 D, which is in good agreement with the experimentally observed value of 0.64 D, thus suggesting that the parametrization yields reasonable accuracy. The calculated S_1–Q_y coupling, when using exact lycopene geometries and heteroatom parametrization is 27.6 cm^{-1}, which is much larger than the calculated $2A_g^-$–Q_y coupling of 1.6 cm^{-1} for the polyene analog with $n = 11$. For peridinin, an experimental estimate of the transition dipole moment is not available. The calculated S_1–Q_y coupling for the Per614–Chl601 system, depicted in Figure 4, is 185.5 cm^{-1}, which is more than 10 times larger than the calculated $2A_g^-$–Q_y coupling of 14.7 cm^{-1} for a perfect polyene with $n = 9$ fitted into the Per614 geometry.

The different sizes of the symmetry breaking effects for peridinin and lycopene can be rationalized by analyzing the prerequisites for symmetry breaking. Carotenoids do not exhibit the symmetries of perfect polyenes, thus rendering transitions allowed that are forbidden in the perfectly symmetric case. In order for the S_1 state to become significantly allowed, both the alternancy symmetry and the geometrical C_{2h} symmetry need to be broken. The alternancy symmetry is broken in all carotenoids, due to non-hydrogen sidegroups attached to the carbons of the conjugated π-electron system. However, some carotenoids retain an approximate C_{2h} symmetry in solution. For example, lycopene and rhodopin glucoside both show a C_{2h} symmetrical arrangement of their methyl groups, from which follows that their S_1 state is forbidden in solution at low temperatures, where vibrational fluctuations are small. In protein environments and at higher temperatures, this C_{2h} symmetry is broken either through the static fixation in a bent shape or through dynamic fluctuations of the protein. For approximately C_{2h} symmetrical carotenoids, the transition dipole moment of the S_1 state is thus induced only by the distortions from the ideal polyene geometry. For lycopene, the static distortions through the ligation to the protein are small as witnessed by the straight shape of lycopene in the crystal structure. Therefore, the effect of symmetry breaking on the couplings and transition dipole moments is small.

In contrast to lycopene, for peridinin the C_{2h} symmetry is broken in multiple ways already in solution through the non-symmetrical arrangements of methyl groups and the carbonyl group connected to the conjugated system. Therefore, the effect of symmetry breaking on couplings and transition dipole moments is expected to be larger than in lycopene, consistent with calculations. Since the authors could not test the parametrization of the carbonyl group ring, they investigated in Damjanović et al. (2000b) the effect of symmetry breaking through the methyl groups seperately from the effect through the carbonyl group. It was found that both the methyl groups and the carbonyl group have a significant effect in enhancing the electronic couplings.

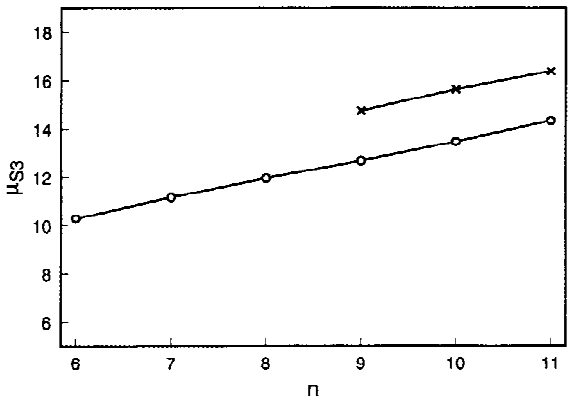

Figure 5. Transition dipole moments in D for the S_3 ($1B_u^+$) state. the circles indicate calculated values for polyenes with n conjugated double bonds, the crosses indicate measured values for neurosporene ($n = 9$), spheroidene ($n = 10$) and lycopene ($n = 11$) as reported in Zhang et al. (2000).

S_3 ($1B_u^+$) state

The optically allowed S_3 state is much more amenable to electronic coupling calculations than S_1, because the drastic differences in couplings between an idealized polyene and a carotenoid with broken symmetries, found in case of the S_1 state, do not arise here.

In Figure 5, the calculated transition dipole moments for the $1B_u^+$ state of polyenes with $n = 6$ to $n = 11$ are shown in comparison with the experimentally determined transition dipole moments for neurosporene ($n = 9$), spheroidene ($n = 10$), and lycopene ($n = 11$) (Zhang et al. 2000). The calculated values differ less than 15% from the experimental ones and show the same linear increase with larger n. This correspondence suggests that the $1B_u^+$ state wavefunctions are approximated well.

The $1B_u^+$–Q_x couplings listed in Table 4, evaluated for polyenes with increasing n, increase monotonic-

Table 4. Electronic couplings (in cm^{-1}) between the carotenoid S_3 ($1B_u^+$) and BChl Q_x states calculated for perfect polyenes fitted into the geometries of the lycopene-BChl system in LH 2 from *Rs. molischianum*

n	6	7	8	9	10	11
U_{DA}	83.0	93.3	115.4	118.4	149.5	242.0

ally, but not linearly. This increase partly parallels the observed increase in transition dipole moments with longer conjugated systems, but changes in the geometrical arrangement provide additional effects.

The effect of spectral overlap

S_1 ($2A_g^-$) state

The S_1 state of carotenoids is in resonance with the Q_y excitation of BChls. The energy of the S_1 excited state of carotenoids has been suggested to decrease with the number of double bonds n, following an $\frac{1}{n+1}$ dependence (Tavan and Schulten 1986, 1987). The shift of energy relative to the energy of the absorbing BChl state will result in a difference in spectral overlap. In this section, we investigate the influence of the number of conjugated double bonds on the spectral overlap and, hence, the rate of energy transfer.

The spectra of S_1 emission have recently been measured by steady state fluorescence spectroscopy in an *n*-hexane solution for neurosporene ($n=9$), spheroidene ($n=10$), and lycopene ($n=11$) (Zhang et al. 2000). The measurements were taken at room temperature using the experimental setup described in (Fujii et al. (1998).

Figure 6 shows the normalized S_1 fluorescence spectra for neurosporene, spheroidene, and lycopene. Also shown is the normalized BChl absorption spectrum of the LH 2 complex from *Rs. molischianum*.

Table 5 shows the spectral overlaps between carotenoid S_1 states and monomeric B800 and B850 BChl Q_y excitations. The spectral overlaps were calculated according to Equation 2 using the emission spectra shown in Figure 6. For the absorption spectra, a single Gaussian with a width of 400 cm^{-1} centered around 800 or 850 nm for monomeric B800 and B850 BChls was used. The observed spectral overlaps exhibit no monotonic correlation with the length of conjugated systems. Rather, they peak for spheroidene

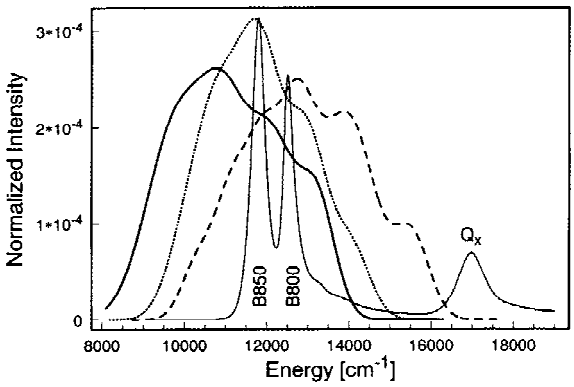

Figure 6. Fluorescence S_1 state spectra reconstructed from spectral deconvolution of the measured spectra reported in (Zhang et al. (2000). Shown are the spectra for neurosporene (dashed line), spheroidene (dotted line), and lycopene (full line). Also shown is the normalized BChl absorption spectrum of the LH 2 complex from *Rs. molischianum* (thin full line).

Table 5. Origin of S_1 emission and spectral overlaps between S_1 emission and the Q_y absorption of monomeric B800 and B850 BChls, J_{B800} and J_{B850}.

Carotenoid (n)	E_{S1} [cm^{-1}]	J_{B800} [10^{-4} cm]	J_{B850} [10^{-4} cm]
Neurosporene (9)	15300	2.40	1.89
Spheroidene (10)	14150	2.34	2.93
Lycopene (11)	13200	2.10	2.66

and decrease for longer and shorter conjugated systems. In order to demonstrate this feature more clearly, we shifted the energy origins for the S_1 emission of the three carotenoids in question to values between 11 000 and 17 000 cm^{-1} and evaluated the spectral overlap with the B850 states. This dependence is displayed in Figure 7. The most striking feature is that the spectral overlap is not a monotonic function of the energy origin, but peaks around 14 000 cm^{-1} for the B850 state (14 700 cm^{-1} for the B800 state). Apparently, nature has optimized the S_1–Q_y spectral overlap for carotenoids in the region between 13 000 cm^{-1} and 15 000 cm^{-1}. Only outside of this window will the spectral overlap decrease strongly and almost linearly. The energy origins for neurosporene, spheroidene, and lycopene with 9–11 conjugated double bonds all fall into this region of high spectral overlap, with the neurosporene being at the border of the window and exhibiting a slightly smaller spectral overlap.

The relative independence of the spectral overlap on the energy origin can be rationalized from Figure 6.

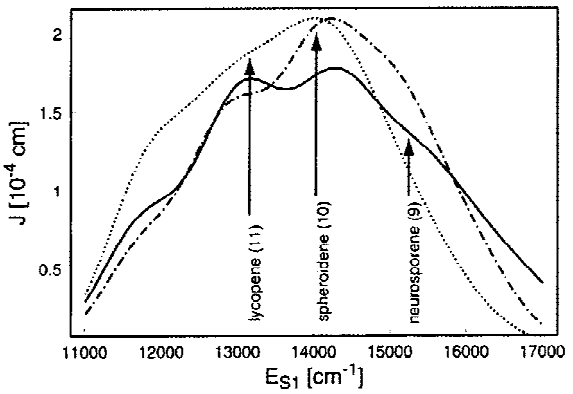

Figure 7. Spectral overlap between the carotenoid S_1 state and the Q_g state of B850 BChl . The spectral overlap was evaluated using the lineshape of neurosporene (full line), spheroidene (broken line) and lycopene (dotted line) emission spectra shifted to the respective energy origins and a single Gaussian with a FWHM of 400 cm^{-1} for the BChl absorption spectra.

The carotenoid emission spectra are very broad compared to the BChl absorption and encompass the BChl absorption spectra for all three carotenoids. The main difference lies in the relative position of the emission maxima to the absorption maxima.

It should be noted that the knowledge of the S_1 emission lineshape provides a more reliable estimate of the spectral overlap compared to earlier calculations that approximated the S_1 emission spectrum with a single Gaussian with a FWHM of 3000 cm^{-1} (Nagae et al. 1993; Krueger et al. 1998b; Damjanović et al. 1999).

Since the energy origins for the carotenoids above have been measured in *n*-hexane, it is possible that they will be shifted in the protein environment. The authors in (Krueger et al. (1999) have measured the S_1 state emission of spheroidene in the protein environment and assigned an energy origin E_{S1} = 13 900 cm^{-1}. This value results in less than 5% difference in spectral overlap with B850 BChl and about 4% difference in spectral overlap with B800 BChl compared to spheroidene with E_{S1} = 14 150 cm^{-1}.

Another uncertain parameter in the calculation of the spectral overlap is the lineshape of the BChl states. The presented results are robust against changes in the width of the BChl absorption. Decreasing the homogenous width of the BChl absorptions by a factor of two results in less than 3% changes of the spectral overlap. However, in calculating the spectral overlap with the B850 BChls, one has to consider that the B850 Q_y excitations form delocalized exciton states. Rather than using the absorption spectrum of a single BChl, one has to calculate the exciton energy density of the various B850 exciton states in order to evaluate the overlap integral. Assuming weak exciton-phonon coupling, one can approximate the exciton density as a sum of Gaussians with centers at energies in the range between 11 500 cm^{-1} and 14 000 cm^{-1} (Hu et al. 1998b); for stronger exciton-phonon couplings, the exciton energy density can be calculated as suggested in Mukai et al. (1999). Each exciton state is characterized by a different electronic coupling to the carotenoids. The effect of the delocalized exciton is thus to open additional potential pathways for excitation transfer. However, unlike for B800 → B850 excitation transfer, where higher exciton states are instrumental for fast transfer, the effect of BChl exciton states increases spectral overlaps with carotenoids only marginally (Damjanović et al. 1999) and is not important for enhancing excitation transfer rates.

The spectral overlap is directly proportional to the rate of excitation transfer. The main conclusion from the discussion in this section is that no monotonic relation between the length of conjugated system and the spectral overlap exists for carotenoids with 9–11 conjugated double bonds. If one assumes that 75% of excitation is transferred to the B850 BChls, and 25% to the B800 BChl, as suggested in Kramer et al. (1984) and Shreve et al (1991) then the rate of excitation transfer decreases by about 25% from spheroidene ($n = 10$) to neurosporene ($n = 9$), and decreases by about 15% from spheroidene ($n = 10$) to lycopene ($n = 11$). While these effects are noticable, they do not suggest the spectral overlap as a dominant factor in explaining transfer efficiencies through the S_1 state, in particular when comparing transfer through the S_1 state of peridinin ($n = 9$) with the much less efficient transfer through the S_1 state of lycpopene ($n = 11$).

S_3 ($1B_u^+$) state

Unlike for the S_1 state, the spectral overlaps for the S_3 state of the three carotenoids discussed exhibit a monotonic increase with increasing *n*, as can be seen from Table 6. This is because the Q_x state absorption is located at the lower edge of the respective emission spectra. The spectral overlap with the S_3 state will increase for carotenoids with up to 13 conjugated double bonds where the S_3 emission then encompasses the Q_x absorption, similar to the situation for S_1-B850(Q_y) spectral overlap for shorter carotenoids, and will decrease for even longer conjugated systems.

Table 6. Origin E_{S3} of S_3 ($1B_u^+$) emission and spectral overlap J between S_3 emission and the Q_x absorption BChls

Carotenoid (n)	E_{S3} [cm^{-1}]	J [10^{-4} cm]
Neurosporene (9)	21135	0.27
Spheroidene (10)	20330	0.76
Lycopene (11)	19420	1.45

Table 7. S_1 ($1A_g^-$) state lifetimes as measured in Zhang et al. 2000). The effect of the decrease in lifetimes with increase in n on the efficiency of $S_1 \rightarrow Q_y$ excitation transfer is shown in the last two columns, assuming a constant transfer time constant of 10 or 20 ps for all three carotenoids

Carotenoid (n)	τ_{S1} [ps]	η for $\tau_{ET} = 10$ ps	η for τ_{ET}=20 ps
Neurosporene (9)	21.2	68%	51%
Spheroidene (10)	9.3	48%	32%
Lycopene (11)	4.7	32%	19%

For the carotenoids in question, the transfer rate decreases by about a factor two when the number of conjugated double bonds increases by one. This systematic effect is a factor that has to be considered when explaining $S_3 \rightarrow Q_x$ transfer efficiencies, as suggested earlier in Frank et al. (1997) and Desamero et al (1998). However, one has to keep in mind that the newly discovered S_2 ($1B_u^-$) opens a new pathway for transfer. Depending on how fast the S_2 state becomes populated after initial excitation of the S_3 state, transfer to the BChl Q_x state may not originate from the S_3, but rather from the S_2 state, resulting in a very different dependence of spectral overlaps with increasing n.

The effect of lifetimes

S_1 ($2A_g^-$) state

Competing with excitation energy transfer from a carotenoid state is internal conversion from this state to a lower-lying state. The internal conversion rate can be estimated by measuring the lifetime of excited states in solution, where the excitation transfer processes cannot occur. One makes here the assumption that the internal conversion rate in the protein environment is the same as in solution.

The S_1 ($2A_g^-$) lifetime has been measured through transient absorption spectroscopy in n-hexane (Zhang et al. 2000). As stated in Table 7, the lifetime decreases from 21.2 ps for neurosporene ($n=9$) to 9.3 ps for spheroidene ($n=10$) to 4.7 ps for lycopene ($n=11$). This decrease of lifetimes with an increase of n is expected from the energy gap law (Englman and Jortner 1970) because the S_1–S_0 energy gap decreases with an increase of n (cf. Table 5). Regarding the mechanism of internal conversion, it has been shown that S_1–S_0 internal conversion is facilitated by vibronic coupling between these states through the totally symmetric C=C stretching vibration (Macpherson and Gillbro 1998; Zhang et al. 1998; Nagae et al. 2000).

The efficiency for transfer through the S_1 state can be evaluated according to:

$$\eta_{S1} = \frac{\tau_{S1}}{\tau_{S1} + \tau_{ET}} , \qquad (13)$$

where τ_{S1} is the S_1 state lifetime in the absence of excitation transfer and $\tau_{ET} = 1/k_{DA}$ is the time constant of excitation transfer. In order to estimate the effect of this increase in lifetimes on the transfer efficiency seperately from other effects, we assume a constant rate of excitation transfer for all three carotenoids. Since transfer through the S_1 state has a low efficiency in lycopene, the time constant for excitation transfer should be longer than 4.7 ps. If we assume a constant τ_{ET} of 10 ps for all three carotenoids, the transfer efficiency decreases from 68% (neurosporene) to 48% (spheroidene) to 32% (lycopene), and for τ_{ET} = 20 ps, the efficiency decreases from 51% to 32% to 19% (cf. Table 7). The shortening of lifetimes thus has a significant effect on the transfer efficiencies from the S_1 state, decreasing the efficiencies with increasing n.

S_3 ($1B_u^+$) state

Analogous to the S_1 state, it has been expected that the S_3 ($1B_u^+$) $\rightarrow$ S_1 internal conversion time increases with an increase of n because the energy gap between these two states decreases (Frank et al. 1997).

In addition to the direct measurement of the spheroidene S_3 lifetime in n-pentane by fluorescence up-conversion (Ricci et al. 1996), the S_3 lifetimes of neurosporene and lycopene in n-hexane have recently been determined by time-resolved absorption spectroscopy (Zhang et al., unpublished results). Surprisingly, the S_3 lifetime is found to decrease in the order neurosporene ($n=9$) 320 fs > spheroidene

($n = 10$) 250 fs > lycopene ($n = 11$) 130 fs. This decrease in lifetimes for an increase in n will result in a decrease of efficiencies for transfer from the S_3 state.

It has been noted earlier that vibronic coupling between the S_3 ($1B_u^+$) and S_1 ($2A_g^-$) state should be forbidden because of the different alternancy symmetries of the states (+ vs. −) and that an additional optically forbidden state between the S_3 and S_1 state can be involved in mediating S_3 to S_1 relaxation (Watanabe and Karplus 1993; Kuki et al. 1994). On the basis of renormalized CI calculations, it has been predicted that a $1B_u^-$ state should be located between the S_3 ($1B_u^+$) and S_1 ($2A_g^-$) states for polyenes with $n > 6$ and that the $1B_u^-$ energy should decrease more rapidly than that of the S_3 ($1B_u^+$) or S_1 ($2A_g^-$) state with an increase in n (Tavan and Schulten 1979, 1986, 1987).

The predicted $1B_u^-$ state has indeed been experimentally identified by measurements of resonance-Raman excitation profiles which place it at 17 680 cm^{-1} for spheroidene and 15 770 cm^{-1} for lycopene (Sashima et al. 1999, 2000). For lack of measurement of the $1B_u^-$ state energy for neurosporene, we use the value for mini-β-carotene (19 600 cm^{-1}), which also has nine conjugated double bonds (Sashima et al. 2000) Very recently, the $1B_u^+$ and $1B_u^-$ states have also been observed through a second experimental technique, near-infrared time-resolved absorption spectrosopy, for various carotenoids (Zhang and Koyama, unpublished results).

Figure 8 shows the energy diagram including the newly discovered $1B_u^-$ state for the three carotenoids mini-β-carotene, spheroidene and lycopene. It can be seen that the energy gap between the $1B_u^-$ and $2A_g^-$ states decreases with an increase in n. If one assumes that $1B_u^-$ to $2A_g^-$ internal conversion is the time-determining step in $1B_u^+$ to $2A_g^-$ internal conversion, then the observed decrease in $1B_u^+$ lifetimes is again reconciled with the energy gap law. Since $1B_u^-$ and $2A_g^-$ have the same alternancy symmetry, vibronic coupling between these states is allowed and a b_u-type normal mode has been identified that can mediate vibronic coupling between these two states (Sashima et al. 1999).

The mechanism of internal conversion between the $1B_u^+$ and $1B_u^-$ state remains an open question. It has been suggested that the forbiddenness of the + − − vibronic transition is lifted because of the near degeneracy of the two states. However, for longer carotenoids the $1B_u^+ \rightarrow 1B_u^-$ energy gap widens and becomes larger than the $1B_u^-$ to $2A_g^-$ energy gap for lycopene ($n = 11$) and longer carotenoids. In this case, the $1B_u^+ \rightarrow 1B_u^-$ transition cannot be faster than the $1B_u^- \rightarrow 2A_g^-$ transition by virtue of the energy gaps. It has to be studied whether other reasons can be found that corroborate the suggestion that $1B_u^+ \rightarrow 1B_u^-$ internal conversion occurs extremely fast (on the order of tens of fs) and is then followed by a slower (on the order of a few hundreds of fs) $1B_u^- \rightarrow 2A_g^-$ internal conversion.

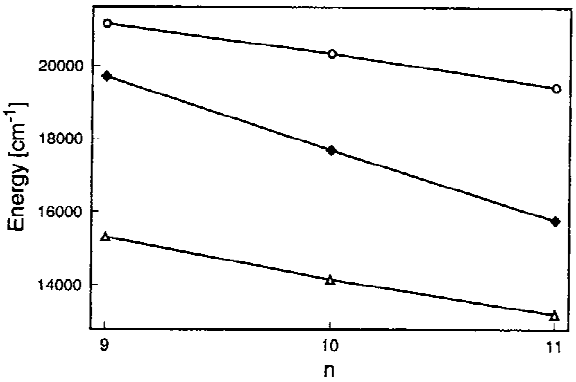

Figure 8. Energy origins of the S_3 ($1B_u^+$) (open circles), S_2 ($1B_u^-$) (filled diamonds), and S_1 ($2A_g^-$) (open triangles) states from neurosporene ($1B_u^+$,$2A_g^-$) and mini-β-carotene ($1B_u^-$), both $n = 9$, spheroidene ($n = 10$) and lycopene ($n = 11$). All states have been directly measured in experiments as reported in the text, showing that the old energy diagram of carotenoids with only $1B_u^+$ and $2A_g^-$ states as low-lying excited states involved in energy transfer will have to be revised. With an increase in n, the $2A_g^-$ state energy decreases slightly more rapidly than the $1B_u^+$ energy (difficult to see, cf. Tables 5 and 6) while the $1B_u^-$ energy decreases clearly more rapidly than that of the two other states.

Discussion

The light-harvesting process through carotenoids is initiated through absorption into the S_3 ($1B_u^+$) state. In this state, direct excitation transfer to the Q_x state competes with internal conversion to the S_1 ($2A_g^-$) state, involving likely the S_2 ($1B_u^-$) state. The $S_3 \rightarrow Q_x$ excitation transfer speeds up considerably with an increase in the number of conjugated double bonds. From our calculations, we predict a transfer time ratio of 20:5:1 for n = 9:10:11. The shortening in transfer times is controlled mainly by the increase in spectral overlaps (see 'S_3 ($1B_u^+$) state' section) and, secondarily, by the increase in electronic couplings (see 'S_3 ($1B_u^+$) state' section). Assuming a transfer time of 200 fs for spheroidene as suggested in Trautmann et

al. (1990) and Shreve et al. (1991), our calculations predict transfer times of 900 fs for neurosporene and peridinin ($n = 9$) and 40 fs for lycopene and rhodopin glucoside ($n = 11$). The latter prediction is in reasonable agreement with the measured transfer time of 63 fs for rhodopin glucoside in LH 2 from *Rps. acidophila* (Macpherson et al. 1998). Since the S_3 lifetime for neurosporene with the same number of double bonds as peridinin is 330 fs, the predicted transfer time of 900 fs is in agreement with the observation that no transfer from the S_3 state occurs in peridinin (Akimoto et al. 1996). For carotenoids with more than nine double bonds, transfer through the S_3 state is on the order of or slightly faster than the internal conversion time, thus opening a new pathway of excitation transfer with an efficiency that is about 50%.

Once energy has relaxed to the S_1 state, again two processes compete, excitation transfer to the Q_y state of BChls, and internal conversion to the ground state. Unlike for the transfer from the S_3 state, no clear trend for the transfer rates with an increase in n can be established. The results of full Coulomb coupling calculations for peridinin and lycopene, based on the crystal structures and including the effect of sidegroup variations, suggest that the controlling factor for the S_1–Q_y electronic couplings is not the length of conjugated system, but the degree of symmetry breaking. The effect of symmetry breaking is to increase the electronic coupling. This effect can be induced either by the use of an asymmetric carotenoid, such as peridinin, in which case the effect is strong, or by geometric distortion of a symmetric carotenoid, such as lycopene, in the protein environment, in which case the effect is weaker. A strong effect of symmetry breaking has been suggested to result from a non-C_{2h}-symmetrical arrangement of the methyl groups in peridinin (Damjanović et al. 2000b). Although the calculated $S_1 \rightarrow Q_y$ couplings for peridinin may be an overestimate, because of the uncertainties in parametrization, the large differences in electronic couplings for the asymmetric peridinin compared to the symmetric lycopene suggest nevertheless that the different symmetries with their effect on the electronic couplings are a dominant factor in explaining why transfer from the S_1 state is highly efficient for peridinin, and not efficient for lycopene.

Compared to the effects of symmetry breaking on electronic couplings which have a quadratic effect on the transfer rates, the effect of spectral overlaps on the $S_1 \rightarrow Q_y$ transfer rates is very small and cannot be considered as a dominant factor. It is interesting to note, though, that the spectral overlap is maximized for carotenoids with n between 9 and 11, the range in which most carotenoids in light harvesting can be found.

It has been suggested that excitation transfer from the carotenoid S_1 state occurs to the Q_x rather than the Q_y state of BChls (Desamero et al. 1998). The rationale for this suggestion was that the efficiency for $S_1 \rightarrow$ BChl transfer is observed to decrease with increasing n and that this behavior can be reconciled with the strong decrease for S_1–Q_x overlap for increasing n. While we do not exclude the $S_1 \rightarrow Q_x$ route, we note that the decrease in efficiencies can arise by virtue of the decrease in S_1–Q_y electronic coupling, a factor that has not been considered in Desamero et al. (1998).

Transfer times for $S_1 \rightarrow Q_y$ transfer have been estimated experimentally for neurosporene, spheroidene, and lycopene by measuring the lifetimes of the S_1 state in *n*-hexane (τ_{S1}) and in the LH 2 protein environment (τ_P) and assuming that the differences in lifetimes are only due to excitation transfer (Zhang et al. 2000). The estimated transfer times, resulting from expression $1/\tau_{ET} = 1/\tau_P - 1/\tau_{S1}$, were 1.4 ps for neurosporene, 2.1 ps for spheroidene, and 12.3 ps for lycopene.

A second factor contributing to the efficiencies of $S_1 \rightarrow Q_y$ transfer is the strong decrease of S_1 lifetimes with increase in n (cf. '$S_3(1B_u^+)$ state' section). The S_1 lifetime for neurosporene ($n = 9$), 22 ps, is almost five times longer than the S_1 lifetime for lycopene ($n = 11$), 4.7 ps. This in itself is a sufficient difference to explain why transfer from the S_1 state in neurosporene is efficient, while it is inefficient in lycopene.

A special situation arises in the case of peridinin, where the S_1 lifetime varies between 7 and 172 ps (Akimot et al. 1996; Frank et al. 2000b), depending on the polarizability of the solvent. Such a strong dependence on the polarizability of the environment had not been observed in S_1 states of carotenoids other than peridinin (Bautista et al. 1996b). The authors in Frank et al. (2000b) compare the spectra and lifetimes of various carotenoids in varying solvent environments in an attempt to elucidate the molecular features responsible for the strong dependence of the lifetime on the environment. They found that the presence of a carbonyl group in conjunction with the conjugated system is required for a strong effect of the environment on the S_1 state lifetime and suggest that the spectral and lifetime changes observed in Frank et al. (2000b) can be explained through the presence of a charge transfer state mixing with the S_1 state. The electron-withdrawing character of the carbonyl group

would, in this model, serve to stabilize the hypothetical charge transfer state and, thus, explain why carotenoids with carbonyl groups show a strong dependence on the solvent polarizability. These results suggest that the carbonyl group in peridinin has a distinct influence on the lifetime and of the S_1 state which goes beyond the symmetry breaking effect on the electronic couplings presented in this manuscript.

Summarizing this discussion, we note that the experimentally observed overall Car → Chl transfer efficiencies can be explained in systems for which theoretical and experimental data are available. The overall transfer efficiency is determined mainly by the efficiency of transfer through the S_1 state. Light-harvesting systems with a low overall efficiency, such as LH 2 from *Rs. molischianum* and *Rps. acidophila* employ long, symmetric polyenes (lycopene, rhodopin glucoside). Their resulting small S_1–Q_y electronic couplings and short S_1 lifetimes render transfer through the S_1 state inefficient. Excitation transfer in these light-harvesting systems occurs through the S_3 → Q_x pathway. Because of the short S_3 lifetime, the efficiency of this transfer is low.

In contrast, systems with near unit transfer efficiencies, such as PCP from *A. carterae* and LH 2 from *Rb. sphaeroides* G1C, employ short ($n = 9$) polyenes (peridinin, neurosporene). In case of the symmetric neurosporene, the long S_1 lifetimes renders transfer through the S_1 state efficient. In peridinin, the effect of symmetry breaking, through asymmetrical arrangement of methyl sidegroups and the presence of a carbonyl group, vastly increases S_1–Q_y electronic couplings. This increase, in conjunction with an additional effect of the carbonyl group on the spectroscopic properties of peridinin renders transfer through the S_1 state efficient.

A particular interesting system is LH 2 from *Rb. sphaeroides* 2.4.1, which employs the carotenoid spheroidene ($n = 10$). Its S_1 lifetime is only a factor 2 longer than the lycopene S_1 lifetime in *Rs. molischianum* and, therefore, not sufficient as an explanation for the near unit efficiency observed in *Rb. sphaeroides* 2.4.1 as opposed to the 50% efficiency in the lycopene–BChl system in *Rs. molischianum*. The conjugated systems of neurosporene, spheroidene and lycopene are shown in Figure 9. An inspection of the spheroidene structure shows that spheroidene (as well as neurosporene) exhibits a non C_{2h}-symmetrical arrangement of its methyl sidegroups, unlike lycopene. On the basis of the electronic coupling calculations reviewed here, we suggest that this symmetry

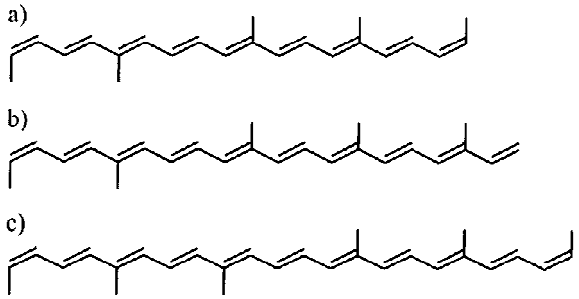

Figure 9. Structure of conjugated systems with methyl sidegroups of neurosporene, spheroidene, and lycopene. The C_{2h} symmetry is broken for neurosporene and spheroidene, since five methyl sidegroups cannot be arranged such that the structure is invariant under rotation by 180°. In contrast, the six methyl sidegroups on lycopene are arranged in C_{2h} symmetric fashion. Symmetry breaking enhances couplings to the S_1 state, and, thus, excitation transfer rates. The structures suggest that transfer through the lycopene S_1 is slower than through the neurosporene or spheroidene S_1 state, which is consistent with experimental data.

breaking can be a dominant factor in explaining why transfer through the S_1 state is efficient in spheroidene, but not in lycopene. We note that the symmetry properties can provide an explanation for the experimentally estimated S_1 → Q_y transfer times, which are very similar for the equally asymmetrical neurosporene and spheroidene (1.4 ps and 2.1 ps, respectively), but significantly longer for lycopene (12.1 ps). Additional support for this suggestion comes from a reconstitution study (Noguchi et al. 1990), in which the efficiency of Car → Chl transfer was found to drop from 72% to 43% when spheroidene ($n = 10$) was replaced by rhodopin ($n = 11$) in LH1 from *Rb. sphaeroides*, whereas a substitution by neurosporene ($n = 9$) had no effect on the efficiency. Since the conjugated system of rhodopin is identical to that of lycopene, the above mentioned symmetry breaking effect can account for the observed differences in efficiencies.

We caution against conclusions in the absence of structural information. One result from our comparative analysis of electronic couplings with the S_1 state of carotenoids is that the exact geometrical arrangement has a significant effect on the couplings, likely to be more significant than the length of conjugated system or even the symmetry breaking. The strong influence of electronic couplings is consistent with experimental studies that suggested a strong influence of the geometry of the Car–Chl system on transfer efficiencies (Cogdell et al. 1981; Noguchi et al. 1990). While the strong dependence on the geometries may invalidate some of our conclusions and suggestions for

the effect of electronic couplings, it also means that nature can employ this dependence to control energy transfer efficiencies. To say the least, it can be misleading to analyze excitation transfer efficiencies solely on the basis of spectral overlap and lifetimes, assuming that electronic couplings are similiar between different species of light-harvesting systems.

The picture of excitation transfer efficiencies presented in this article is not complete because it does not yet include the function of the newly found S_2 ($1B_u^-$) state. While we have so far only discussed its potential role for accelerating S_3–S_1 internal conversion, it is clear that this state will have a role in understanding $S_3 \rightarrow Q_x$ transfer. If it is true that the S_3 state relaxes within tens of fs into the S_2 state, excitation transfer to the Q_x state may have to be described as originating from the S_2 rather than the S_3 state, or, alternatively, as originating from a mixture of S_3 and S_2 states. However, it is not to be expected that the existence of the S_2 state will significantly speed up transfer to the Q_x state because of its optically forbidden character and likely brief lifetime. Therefore, we conclude that the overall efficiency of transfer is controlled by the factors that increase transfer efficiency trough the S_1 state after internal conversion from S_3 and S_2. However, the S_2 state might be important when the fast $S_3/S_2 \rightarrow Q_x$ transfer pathways are employed, as for example in LH 2 from *Rps. acidophila* or *Rs. molischianum*.

In the present article, we have been concernced with the principles controlling the efficiencies of excitation transfer and brushed over the differences in various light-harvesting systems, focussing mainly on the properties of their carotenoids in a comparatative manner.

Focussing on the specifics of a light-harvesting system from a given species is not only a matter of scientific thoroughness, but also a means to reveal specific strategies by which an individual light-harvesting species has fine-tuned its control of light harvesting through carotenoids. An example of a peculiar light-harvesting strategy can be seen in PCP from *A. carterae*. It has been noted frequently that this light-harvesting protein employs carotenoids as most abundant light absorbers, with a 4:1 ratio between carotenoids and chlorophylls. However, only a study accounting for full Coulomb coupling reveals how well the system is tuned for efficient light absorption. As described in Damjanović et al. (2000b), the absorbing $1B_u^+$ states of each group of four carotenoids in contact with one Chl are strongly coupled among each other, forming delocalized excitations over all four carotenoids. This excitonic state resides on one to three out of the four carotenoids, excluding peridinin 612, for which the exciton density is distinctly lower than for the other carotenoids. Following the fast internal conversion from the $1B_u^+$ to the $2A_g^-$ state, the majority of S_1 excitation will, therefore, be trapped on carotenoids other than peridinin 612, regardless of which carotenoid absorbed the energy initially. It is this peridinin for which the $2A_g^-$-Q_y electronic coupling is weakest. The exclusion of peridinin 612 from the light-harvesting route, achieved by a meticulous organization of quantum mechanical states, is thus enhancing the overall light-harvesting efficiency of PCP.

Similar specific strategies may be found for other species, when one tries to reconcile experimental observations with theoretical predictions of excitation transfer pathways for an individual light harvesting system. This remains to be done in particular for the LH 2 system from *Rps. acidophila*, for which a wealth of experimental data is available as reviewed in Cogdell et al. (1999). Open questions are, e.g. the role of the B800 BChls as a mediator of excitation transfer from carotenoids to B850 BChls and the role of the larger bending of rhodopin glucoside in LH 2 from *Rps. acidophila* compared to the otherwise very similar lycopene in LH 2 from *Rs. molischianum*.

In conclusion, we note that nature employs two types of chromophores to harvest the light energy of the sun, chlorophylls and carotenoids. Chlorophylls in light-harvesting systems provide the primary link to the final acceptors of excitation energy, the special pair of chlorophylls in the photosynthetic reaction center. Because of the choice of identical molecules, spectral overlap between light-harvesting and special pair chlorophylls is very high. However, the absorption maximum of chlorophylls lies in the red or near-infrared, while the emission maximum of the sun lies in the yellow-green. In order to harvest energy close to the region of maximal emission of the sun, nature recruited carotenoids as secondary chromophores. An immediate problem arises: Because of their high excitation energy, carotenoids are out of resonance with the chlorophyll excitation, which results in a small spectral overlap and, thus, inefficient excitation transfer to the chlorophylls. Fortunately, carotenoids exhibit an electronic structure that overcomes this problem: They utilize a high-lying excitation, which efficiently absorbs light in the yellow-green, but is extremely short lived, relaxing into an optically forbidden lower-lying

state in resonance with the chlorophyll excitation. The studies reviewed in this article have shown that Car → Chl transfer achieves only high efficiency when both the optically allowed and the optically forbidden state are used as transfer gateways. For the optically forbidden state to serve as a strong transfer gateway, its electronic coupling to the chlorophyll state must be sufficiently strong. One factor that controls the electronic coupling strength and thus the transfer efficiency is the symmetry of carotenoids. Nature can enhance electronic couplings by employing carotenoids with functional sidegroups that break the carotenoid symmetry.

A full understanding of the light-harvesting function of carotenoids requires not only knowledge of the chemical structure of the employed carotenoids, but also knowledge of the exact geometrical arrangement of the carotenoids-chlorophyll system. The advances in structural biology, resulting in the discovery of more and more light-harvesting systems, will permit a comparison of the strategies employed by different systems in the competition for efficient harvesting of the sunlight, one of the most ancient and fundamental processes of all life on earth.

Acknowledgements

The authors would like to express their thanks to Richard J. Cogdell and Harry Frank for helpful comments. This work was supported by grants from the National Science Foundation (NSF BIR 94-23827 EQ and NSF BIR-9318159), the National Institutes of Health (NIH PHS 5 P41 RR05969-04) and the Roy J. Carver Charitable Trust.

References

Akimoto S, Takaichi S, Ogata T, Nishimura Y, Yamazaki I and Mimuro M (1996) Excitation energy transfer in carotenoid-chlorophyll protein complexes probed by femtosecond fluorescence decays. Chem Phys Lett 260: 147–152

Angerhofer A, Cogdell R and Hipkins M (1986) A spectral characterization of the light-harvesting pigment–protein complexes from *Rhodopseudomonas acidophila*. Biochim Biophys Acta 848: 333–341

Angerhofer A, Bornhäuser F, Gall A and Cogdell R (1995) Optical and optically detected magnetic resonance investigation on purple bacterial antenna complexes. Chem Phys 194: 259–274

Bautista J, Hiller R, Sharples F, Gosztola D, Wasielewski M and Frank H (1999a) Singlet and triplet transfer in the Peridinin-Chlorophyll *a*-protein from *Amphidinium carterae*. J Phys Chem A 103: 2267–2273

Bautista JA, Connors RE, Raju BB, Hiller RG, Sharples FP, Gosztola D, Wasielewski M and Frank HA (1999b) Exited state properties of peridinin: Observation of solvent dependence of the lowest excited singlet state lifetime and spectral behavior unique among carotenoids. J Phys Chem B 103: 8751–8758

Chadwick B, Zhang C, Cogdell R and Frank H (1987) The effects of lithium dodecyl sulfate and sodium borohydride on the absorption spectrum of the B800–850 light harvesting complex from *Rhodopseudomonas acidophila* 7750. Biochim Biophys Acta 893: 444–451

Christensen R (1999) The electronic states of carotenoids. In: Frank H, Young A, Britton G and Cogdell R (eds) The Photochemistry of Carotenoids, pp 137–159. The Netherlands

Cogdell R, Hipkins M, MacDonald W and Truscott T (1981) Energy transfer between the carotenoid and the bacteriochlorophyll within the B-800–850 light-harvesting pigment–protein complex of *Rhodopseudomonas sphaeroides*. Biochim Biophys Acta 634: 191–202

Cogdell R, Andersson P and Gillbro T (1992) Carotenoid singlet states and their involvement in photosynthetic light-harvesting pigments. J Photochem Photobiol B 15: 105–112

Cogdell R, Isaacs N, Howard T, McLuskey K, Fraser N and Prince S (1999) How photosynthetic bacteria harvest solar energy. J Bacteriol 181: 3869–3879

Cory MG, Zerner MC, Hu X and Schulten K (1998) Electronic Excitations in Aggregates of Bacteriochlorophylls. J Phys Chem B 102(39): 7640–7650

Damjanović A, Ritz T and Schulten K (1999) Energy transfer between carotenoids and bacteriochlorophylls in a light harvesting protein. Phys Rev E 59: 3293–3311

Damjanović A, Ritz T and Schulten K (2000a) Excitation energy trapping by the reaction center of *Rhodobacter sphaeroides*. Int J Quantum Chem 77: 139–151

Damjanović A, Ritz T and Schulten K (2000b) Excitation transfer in the peridinin-chlorophyll-protein of *Amphidinium carterae*. Biophys J 79: 1695–1705

Desamero R, Chynwat V, Van der Hoef I, Jansen F, Lugtenburg J, Gosztola D, Wasielewski M, Cua A, Bocian D and Frank H (1998) Mechanism of energy transfer from carotenoids to bacteriochlorophyll: Light-harvesting by carotenoids having different extents of π-electron conjugation incorporated in the B850 antenna complex from the carotenoidless bacterium *Rhodobacter sphaeroides* R-26.1. J Phys Chem B 102: 8151–8162

Dexter D (1953) A theory of sensitized luminescence in solids. J Chem Phys 21: 836–850

Englman R and Jortner J (1970) The energy gap law for radiationless transitions in large molecules. Mol Phys 18: 145–164

Farshoosh R, Chynwat V, Gebhard R, Lugtenburg J and Frank H (1994) Triplet energy transfer between bacteriochlorophyll and carotenoids in B850 light-harvesting complexes of *Rhodobacter sphaeroides* R-26.1. Photosynth Res 42: 157–166

Farshoosh R, Chynwat V, Gebhard R, Lugtenburg J and Frank H (1997) Triplet energy transfer between the primary donor and carotenoids in *Rhodobacter sphaeroides* R-26.1 reaction center incorporated with spheroidene analogs having different extent of π-electron conjugation. Photochem Photobiol 66: 97–104

Förster T (1948) Zwischenmolekulare Energiewanderung und Fluoreszenz. Ann Phys (Leipzig) 2: 55–75

Förster T (1965) Delocalized Excitation and Excitation Transfer, pp. 93–137. Academic Press, New York

Frank H (1993) Carotenoids in photosynthetic bacterial reaction centers: structure, spectroscopy, and photochemistry. In: The Photosynthetic Reaction Center, Vol. 2, pp 221–237.

Frank H, Bautista J, Josue J and Young A (2000a) Mechanism of nonphotochemical quenching in green plants: Energies of the lowest excited singlet states of violaxanthin and zeaxanthin. Biochemistry 39: 2831–2837

Frank H, Chynwat V, Desamero R, Farshoosh R, Erickson J and Bautista J (1997) On the photophysics and photochemical properties of carotenoids and their role as light-harvesting pigments in photosynthesis. Pure Appl Chem 68: 2117–2124

Frank H and Cogdell R (1996) Carotenoids in photosynthesis. Photochem Photobiol 63: 257–264

Frank HA, Bautista JA, Josue J, Pendon Z, Hiller RG, Sharples FP, Gosztola D and Wasielewski MR (2000b) Effect of the solvent environment on the spectroscopic properties and dynamics of the lowest excited states of carotenoids. J Phys Chem B 104: 4569–4577

Freer A, Prince S, Sauer K, Papiz M, Hawthornthwaite-Lawless A, McDermott G, Cogdell R and Isaacs N (1996) Pigment–pigment interactions and energy transfer in the antenna complex of the photosynthetic bacterium *Rhodopseudomonas acidophila*. Structure 4: 449–462

Fujii R, Onaka K, Kuki M, Koyama Y and Watanabe Y (1998) The A_g^- energies of all-trans-neurosporene and spheroidene as determined by fluorescence spectroscopy. Chem Phys Lett 288: 847–863

Gillbro T, Cogdell RF and Sundström V (1988) Energy transfer from carotenoid to bacteriochlorophyll a in the B800-820 antenna complexes from *Rhodopseudomonas acidophila* strain 7050. FEBS Lett 235: 169–172

Herek J, Polivka T, Pullerits T, Fowler G, Hunter C and Sundstrom V (1998) Ultrafast carotenoid band shifts probe structure and dynamics in photosynthetic antenna complexes. Biochem 37: 7057–7061

Hofmann E, Wrench P, Sharples F, Hiller R, Welte W and Diederichs K (1996) Structural basis of light harvesting by carotenoids: peridinin–chlorophyll-protein from *Amphidinium carterae*. Science 272: 1788–1791

Hu X, Ritz T, Damjanović A and Schulten K (1997) Pigment organization and transfer of electronic excitation in the purple bacteria. J Phys Chem B 101: 3854–3871

Hudson B and Kohler B (1972) Chem Phys Lett 14: 299–304

Humphrey WF, Dalke A and Schulten K (1996) VMD – visual molecular dynamics. J Mol Graphics 14: 33–38

Koepke J, Hu X, Münke C, Schulten K and Michel H (1996) The crystal structure of the light harvesting complex II (B800–850) from *Rhodospirillum molischianum*. Structure 4: 581–597

Koyama Y, Kuki M, Andersson P and Gillbro T (1996) Singlet excited states and the light-harvesting function of carotenoids in bacterial photosynthesis. Photochem Photobiol 63: 243–256

Kramer H, Van Grondelle R, Hunter CN, Westerhuis W and Amesz J (1984) Pigment organization of the B800–850 antenna complex of *Rhodopseudomonas sphaeroides*. Biochim Biophys Acta 765: 156–165

Krueger B, Scholes G, Jimenez R and Fleming G (1998a) Electronic excitation transfer from carotenoid to bacteriochlorophyll in the purple bacterium *Rhodopseudomonas acidophila*. J Phys Chem B 102: 2284–2292

Krueger BP, Scholes GD and Fleming GR (1998b) Calculation of couplings and energy-transfer pathways between the pigments of LH2 by the *ab initio* transition density cube method. J Phys Chem B 102: 5378–5386

Krueger B, Scholes G, Gould I and Fleming G (1999) Carotenoid mediated B800–B850 coupling in LH2. Phys Chem Comm 8: 9/03172C.

Kuki M, Nagae H, Cogdell R and Koyama Y (1994) Solvent Effect on spheroidene in nonpolar and polar solutions and the environment of spheroidene in the light-harvesting complexes of *Rhodobacter sphaeroides* 2.4.1 as revealed by the energy of the (1)A(g)(−)B-1(U)+ absorption and the frequencies of the vibronically coupled C=C stretching Raman lines in the (1)A(G)(−) And 2(1)A(G)(−) states. Photochem Photobiol 59: 116

Macpherson A and Gillbro T (1998) Solvent dependence of the ultrfast S_2 -S_1 internal conversion rate of β-carotene. J Phys Chem A 102: 5049–5058

Macpherson AM, Arellano JB, Fraser NJ, Cogdell RJ and Gillbro T (1998) Ultrafast energy transfer from rhodopin glucoside in the light harvesting complexes of *Rps. acidophila*. In: Garab G (ed) Photosynthesis: Mechanism and Effects, Vol 1, pp 9–14. Kluwer Academic Publishers, Dordrecht, The Netherlands

McDermott G, Prince S, Freer A, Hawthornthwaite-Lawless A, Papiz M, Cogdell R and Isaacs N (1995) Crystal structure of an integral membrane light-harvesting complex from photosynthetic bacteria. Nature 374: 517–521

McWeeny R (1992) Academic Press, London

Mimuro M, Nagashima U, Takaichi S, Nishimura Y, Yamazaki I and Katoh T (1992) Molecular structure and optical properties of carotenoids for the *in vivo* energy transfer function in the algal photosynthetic pigment system. Biochim Biophys Acta 1098: 271–274

Mukai K, Abe S and Sumi H (1999) Theory of rapid excitation-energy transfer from B800 to optically-forbidden exciton states of B850 in the antenna system LH 2 of Photosynthetic purple bacteria. J Phys Chem B 103: 6096–6102

Nagae H, Kakitani T, Katohi T and Mimuro M (1993) Calculation of the excitation transfer matrix elements between the S_2 or S_1 state of carotenoid and the S_2 or S_1 state of bacteriochlorophyll. J Chem Phys 98: 8012–8023

Nagae H, Kuki M, Zhang J-P, Sashima T, Mukai Y and Koyama Y (2000) Vibronic coupling through the in-phase C=C stretching mode plays a major role in the $2A_g^-$ -to-$1A_g^-$ internal conversion of all-*trans*-β-carotene. J Phys Chem A 104: 4155–4166

Naqvi KR (1980) The mechanism of singlet-singlet excitation energy transfer from carotenoids to chlorophyll. Photochem Photobiol 31: 523–524

Noguchi T, Kolaczkowski S, Gärtner W and Atkinson GH (1990) Resonance Raman spectra of 13-demethylretinal bacteriorhodopsin and of a picosecond bathochromic photocycle intermediate. J Phys Chem 94: 4920–4926

Polivka T, Herek J, Zigmantas D, Akerlund H-E and Sundström V (1999) Direct observation of the (forbidden) S_1 state in carotenoids. Proc Natl Acad Sci USA 96: 4914–4917

Ricci M, Bradforth SE, Jimenez R and Fleming GR (1996) Internal conversion and energy transfer dynamics of spheroidene in solution and in the LH-1 and LH-2 light-harvesting complexes. Chem Phys Lett 259: 381–390

Ritz T, Damjanović A and Schulten K (1998a) Light-harvesting and photoprotection by carotenoids: Structure-based calculations for photosynthetic antenna systems. In: Garab G (ed) Photosynthesis: Mechanisms and Effects (Proceedings of the XIth International Congress on Photosynthesis), Vol 1, pp 487–490. Kluwer Academic Publishers, Dordrecht, The Netherlands

Ritz T, Hu X, Damjanović A and Schulten K (1998b) Excitons and excitation transfer in the photosynthetic unit of purple bacteria. J Luminescence 76–77: 310–321

Sashima T, Shiba M, Hashimoto H, Nagae H and Koyama Y (1998) The A_g^- energy of crystalline all-trans-spheroidene as determ-

inded by resonance-Raman excitation profiles. Chem Phys Lett 290: 36–42

Sashima T, Nagae H, Kuki M and Koyama Y (1999) A new singlet-excited state of all-*trans*-spheroidene as detected by resonance-Raman excitation profiles. Chem Phys Lett 299: 187–194

Sashima T, Koyama Y, Yamada T and Hashimoto H (2000) The $1B_u^-$ and $2A_g^-$ energies of lycopene, β-carotene and Mini-9-β-carotene as determined by resonance-Raman excitation profile: Dependence of the $1B_u^-$-state energy on the conjugation length. J Phys Chem B 104: 5011–5019

Scholes G, Gould I, Cogdell R and Fleming G (1999) *Ab initio* molecular orbital calculations of electronic couplings in the LH 2 bacterial light-harvesting complex of *Rps. acidophila*. J Phys Chem B 103: 2543–2553

Scholes G, Harcourt R and Ghiggino K (1995) Rate expressions for excitation transfer. An *ab initio* study of electronic factors in excitation transfer and exciton resonance interactions. J Chem Phys 102: 7302–7312

Scholes GD, Harcourt RD and Fleming GR (1997) Electronic interactions in photosynthetic light-harvesting complexes: The role of carotenoids. J Phys Chem B 101: 7302–7312

Schulten K and Karplus M (1972) On the origin of a low-lying forbidden transition in polyenes and related molecules. Chem Phys Lett 14(3): 305–309

Schulten K, Ohmine I and Karplus M (1976) Correlation effects in the spectra of polyenes. J Chem Phys 64: 4422–4441

Shreve AP, Trautman JK, Frank HA, Owens TG and Albrecht AC (1991) Femtosecond Energy-transfer Processes in the B800-850 Light-harvesting Complex of *Rhodobacter sphaeroides*-2.4.1. Biochim Biophys Acta 1058: 280–288

Sumi H (1999) Theory on rates of excitation-energy transfer between molecular aggregates through distributed transition dipoles with application to the antenna system in bacterial photosynthesis. J Phys Chem B 103: 252–260

Sundstrom V, Pullerits T and Van Grondelle R (1999) Photosynthetic light-harvesting: Reconciling dynamics and structure of purple bacterial LH 2 reveals function of photosynthetic unit. J Phys Chem B 103: 2327–2346

Tavan P and Schulten K (1979) The 2^1A_g–1^1B_u energy gap in the polyenes: An extended configuration interaction study. J Chem Phys 70(12): 5407–5413

Tavan P and Schulten K (1986) The low-lying electronic excitations in long polyenes: A PPP–MRD–CI study. J Chem Phys 85(11): 6602–6609

Tavan P and Schulten K (1987) Electronic excitations in finite and infinite polyenes. Phys Rev B 36(8): 4337–4358

Thrash R, Fang H-B and Leroi G (1979) On the role of forbidden low-lying excited states of light-harvesting carotenoids in photosynthesis. Photochem Photobiol 29: 1049–1050

Trautmann J, Shreve A, Violette C, Frank HA, Owens T and Albrecht A (1990) Femtosecond dynamics of energy transfer in B800–850 light-harvesting complexes of *Rhodobacter sphaeroides*. Proc Natl Acad Sci USA 87: 215–219

Van Grondelle R, Kramer H and Rijgersberg C (1982) Energy transfer in the B800–B850-carotenoid light-harvesting complex of various mutants of *Rhodopseudomonas sphaeroides* and of *Rhodopseudomonas capsulata*. Biochim Biophys Acta 682: 208–215

Watanabe M and Karplus M (1993) Dynamics of molecules with internal degrees of freedom by multiple time-step methods. J Chem Phys 99(10): 8063–8074

Young A and Frank H (1996) Energy transfer reactions involving carotenoids: Quenching of chlorophyll fluorescence. Photochem Photobiol B 36: 3–16

Zhang J-P, Fujii R, Qian P, Inaba T, Mizoguchi T and Koyama Y (2000) Mechanism of the carotenoid-to-bacteriochlorophyll energy transfer via the S_1 state in the LH 2 complexes from purple bacteria. J Phys Chem B 104: 3683–3691

Zhang Z, Huang L, Chi Y-I, Kim KK, Crofts AR, Berry EA and Kim S-H (1998) Electron transfer by domain movement in cytochrome bc_1. Nature 392: 677–684